

Crack simulation and probability analysis using irregular truss structure modeling equivalent to a continuum structure

Won Choi¹, Seongsoo Yoon², JeongJae Lee^{3*}

(1. Dept. of Rural Systems Engineering, College of Agriculture and Life Sciences, Seoul National University, Seoul 151-921, South Korea; 2. Dept. of Agricultural and Rural Engineering, College of Agriculture, Life and Environments Sciences, Chungbuk National University, Chungbuk 362-763, South Korea; 3. Dept. of Rural Systems Engineering, Research Institute of Agriculture and Life Sciences, College of Agriculture and Life Sciences, Seoul National University, Seoul 151-921, South Korea)

Abstract: The problems related to agricultural structure engineering for crack simulation and reliability analysis are complicated because its variables contain wide ranges of mean and standard deviation. This paper describes an integrated model to perform crack simulation and reliability analysis of a continuum structure. The structure is assumed to be under a two-dimensional plane stress and the deformation is infinitesimal. A truss structure model that has the same behaviour as a continuum structure was developed using irregular triangle truss components where each element consists of two hinges with an axial degree of freedom at both of their ends. A Monte-Carlo simulation (MCS) was adopted for the reliability analysis. If the length of one side of the irregular triangle mesh is shorter than the thickness of the structure, the slenderness associated with compressive failure needs to be examined only for the short column. For that reason, the failure criterion suitable for the equivalent truss structure model was established by checking only axial stresses acting on truss members. Since nodes of the equivalent truss structure model for the structural analysis in this study consist of hinges, development of plastic hinges that occurred during crack propagation were not considered in this model. To simulate the development of crack, truss members over allowable stresses of tension or compression among truss members with the largest amount of stress at each completed structural analysis time step were sequentially removed. Since irregular triangle meshes have an uncertainty in themselves to compare with regular meshes, the equivalent truss structure model could describe crack propagation more realistically. The failure probabilities of structures under various loads and boundary conditions had good agreement with the analytical solutions directly solved from the limit state equations expressed in the form of moments.

Keywords: crack simulation, probability analysis, irregular truss structure model, failure criteria, Monte Carlo simulation

DOI: 10.3965/j.ijabe.20171001.2024

Citation: Choi W, Yoon S, Lee J. Crack simulation and probability analysis using irregular truss structure modeling equivalent to a continuum structure. *Int J Agric & Biol Eng*, 2017; 10(1): 234–247.

1 Introduction

Various materials used for constructions of structures

Received date: 2015-06-18

Accepted date: 2016-12-25

Biographies: **Won Choi**, PhD, Assistant professor, research interests: agricultural engineering applications using multiphysics models and especially agricultural structure engineering, Email: fembem@snu.ac.kr; **Seongsoo Yoon**, PhD, Professor, research interests: agricultural architecture, structural design and automation system, Email: yss@cbnu.ac.kr.

***Corresponding author: JeongJae Lee**, PhD, Emeritus professor, research interests: structural and systems engineering. Mailing address: Dept. of Rural Systems Engineering, Research Institute of Agriculture and Life Sciences, College of Agriculture and Life Sciences, Seoul National Univ., 1 Gwanak-ro, Gwanak-gu, Seoul 151-921, South Korea. Tel: +82-2-880-4592, Email: ljj@snu.ac.kr.

have different probability distributions with regard to mean and variance of random variables. Particularly, concrete (mixture of aggregate, sand and cement) has a relatively wider range of variance than steel^[1,2]. Because structure has its own inherent uncertainty, probabilistic approaches such as structural system reliability analysis and stochastic structural analysis were introduced to evaluate structural safety under a variety of circumstances. Depending on how variables are related to loads and resistances are handled, current methods can be classified into the first-order second-moment (FOSM) method, second-order second moment (SOSM) method, probabilistic finite element method (PFEM) and stochastic process (SP)^[3].

The mean-value first-order second-moment (MVFOSM) method is based on a first-order Taylor series expansion of the performance function linearized at the mean values of the random variables. The failure probability can be estimated from the reliability index based on the means (first-order) and variances (second-moment) of the random variables. However, all variables should follow a normal distribution and the approach is not invariant because the failure probability may change depending on the definition of the limit state equation^[4]. The reliability index geometrically means the shortest distance from the origin to the failure region^[5]. The contact point on the failure surface is called the most probable failure point (MPFP)^[6,7]. To obtain the MPFP from the nonlinear limit state equation, the advanced FOSM (AFOSM) which linearizes the equation around the MPFP was suggested by introducing iterative methods for optimization^[4]. Because most engineering problems are related to non-normal distributions, it is necessary to transform them into normal distributions. If probability density functions (PDFs) are given, the Rackwitz-Fiessler equivalent normal transformation can be used^[8,9]. The Rosenblatt transformation is used when joint probability density functions (JPDF) for random variables can be transformed into standard normal distributions for variables^[10,11].

Because the FOSM method does not reflect the curvature characteristics of each limit state equation, the SOSM method based on a second-order Taylor series expansion of the performance function linearized at the mean values of the random variables was introduced^[12]. In the most cases, limit state equations could be approximated by the curvature fitting of second-order reliability method (SORM)^[13-16]. However, the method could sometimes leave noises on the curvature. In this case, the point fitted SORM is an alternative^[17].

The FOSM and SOSM methods are limited in their applications because there is no way to know how an external force applied at a point of a structure affects the whole system when the structure consists of many elements. To overcome this weakness, a finite element method (FEM) was combined with probabilistic approaches. However, because there is a weakness in

which failure modes associated with limit state equations are subject to the opinions of designers, the analysis could produce different results of failure probability. Therefore, the analysis was mainly applied to simple structures rather than complex structures^[18-20] or static frame structures in which the materials have less variance than the components of bulky structures^[4,21].

On the other hand, efforts to find dominant failure modes that affect the entire collapse of a structure have been ongoing. Ang et al.^[22] suggested the basic concept of failure modes and Ishizawa^[23] provided a more rational basis for determining appropriate safety margins. Stevenson et al.^[24] executed system reliability analysis of frame structures using the principle of virtual work and plastic collapse mechanism. Gorman^[25] suggested algorithms to automatically calculate the collapse modes of perfectly elasto-plastic structures. However, the applications of these ideas were limited because the number of failure modes increased exponentially depending on the degree of structural complexity. Ma and Ang^[26] researched the failure modes of frame structures and truss structures using nonlinear programming (NLP), and Moses et al.^[27,28] introduced the incremental loading method (ILM) which would determine failure modes and limit state equations by gradually increasing loads. The branch and bound method to detect the upper bound of failure modes under a failure event tree was suggested. However, the method could not handle simultaneous failure modes because it assumed only gradual failures^[29,30]. A β unzipping method to find failure modes while gradually removing elements with high failure probability was developed^[30]. This method identified the important failure modes very quickly but there was always the possibility of missing out on some important failure modes. Other researchers developed an optimization technique using lower bound theory, and the differences between the upper and lower bound methods were compared^[31]. Simulation based methods^[32-35], linear programming (LP) for detecting failure modes of frame structures^[36], and matrix-based system reliability (MSR) to find important failure modes by using genetic algorithms (GA)^[37] were executed.

Monte-Carlo simulation (MCS) was introduced as an alternative to PFEM approaches which are limited to only simple frame structures. The MCS method, which was developed for nuclear weapon researches in the USA in the 1940's, creates pseudo-random numbers, simulates real situations and finds exact solutions. It is a useful method for those situations where the limit state equations could not be defined in the PFEM or multiple integration methods are required due to an excessive number of probabilistic variables. Most various MCS approaches are carried out to reduce the number of iterative calculations. The important sampling method (ISM) to move the locations of sampling to the boundary regions between safety and failure was suggested by Shinozuka^[7] and Melchers^[38].

Although large-scale complex structures have been constructed, PFEM as a representative method cannot give an accurate evaluation of structural safety. Therefore, additional safety margins are left to the structures. The equivalent truss structure model combined with MCS was developed to directly calculate the failure modes and probabilities, and to significantly reduce computational time.

2 Mathematical model

The equivalent truss structure model was developed to substitute solid structure components based on a continuum mechanism that could not explain failure phenomena effectively. The basic unit of this model is a triangular element consisting of three truss elements with a rotational hinge at both ends of the element. It was assumed that the mesh density and quality are high enough to produce a uniform stress distribution within the triangular domain and to create an equilateral triangle, respectively.

2.1 Stress and strain relationship of triangular plane element

Figure 1a shows the relative locations of the nodes of a triangular plane element under plane stress before and after deformation. If the size of the element is infinitesimal, it can be assumed that the stress distribution within the domain is uniform. If all sides of the element maintain a straight line after the element is deformed, all

displacements within the domain will exhibit a linear relationship between them. Figure 1b shows the displacements of nodes before and after deformation. Based upon the linear assumptions, the displacements u and v can be expressed as:

$$u = a_1 + a_2x + a_3y \tag{1}$$

$$v = a_4 + a_5x + a_6y \tag{2}$$

where, $a_1, a_2, a_3, a_4, a_5,$ and a_6 are the coefficients; x and y are the horizontal and vertical directions of the coordinate system, respectively; u and v are the displacements of the x - and y -axes, respectively.

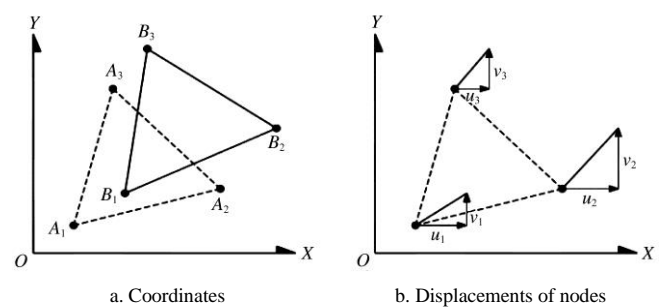


Figure 1 Two-dimensional geometric deformation of a triangular solid element exposed to plane stress

Second order approximation as an expression for the displacements can be used to obtain high quality solutions; however, first order approximations, the results of which are accurate enough for the analysis of the in-plane deformation dealt with in this research, were adopted.

By obtaining the coefficients $a_2, a_3, a_5,$ and a_6 as a form of the coordinates and displacements of nodes 1, 2, and 3 from Equation (1) and (2), the strain-displacement relationships can be rewritten as:

$$\epsilon_x = \frac{(u_1 - u_2)(y_2 - y_3) - (u_2 - u_3)(y_1 - y_2)}{(x_1 - x_2)(y_2 - y_3) - (x_2 - x_3)(y_1 - y_2)} \tag{3}$$

$$\epsilon_y = \frac{(v_1 - v_2)(x_2 - x_3) - (v_2 - v_3)(x_1 - x_2)}{(y_1 - y_2)(x_2 - x_3) - (y_2 - y_3)(x_1 - x_2)} \tag{4}$$

$$\gamma_{xy} = \frac{(u_1 - u_2)(x_2 - x_3) - (u_2 - u_3)(x_1 - x_2)}{(y_1 - y_2)(x_2 - x_3) - (y_2 - y_3)(x_1 - x_2)} + \frac{(v_1 - v_2)(y_2 - y_3) - (v_2 - v_3)(y_1 - y_2)}{(x_1 - x_2)(y_2 - y_3) - (x_2 - x_3)(y_1 - y_2)} \tag{5}$$

where, $x_1, y_1, x_2, y_2, x_3, y_3$ and $u_1, v_1, u_2, v_2, u_3, v_3$ are the x and y coordinates and displacements of nodes 1, 2, and 3, respectively.

2.2 Internal energy of a triangular plane element

Assuming that the thickness of the solid structure in the state of the plane stress is t and the area of the element

is A , the total internal energy of the element can be derived as:

$$U_P = \frac{At}{2} \left[\frac{E}{1-\nu^2} (\varepsilon_x^2 + \varepsilon_y^2 + 2\nu\varepsilon_x\varepsilon_y) + G\gamma_{xy}^2 \right] \quad (6)$$

where, U_P is the internal energy of the plane element; E is the Young's modulus; ν is the Poisson's ratio; G is the shear modulus.

By substituting Equation (6) with Equations (3)-(5), expressed as the coordinates and displacements of each corresponding vertex of a triangular plane element, the total internal energy of the element against the external forces can be represented as:

$$U_P = \frac{At}{2} \left[\frac{E}{1-\nu^2} \left(\frac{\left(\frac{(u_1-u_2)(y_2-y_3)-(u_2-u_3)(y_1-y_2)}{(x_1-x_2)(y_2-y_3)-(x_2-x_3)(y_1-y_2)} \right)^2 + \left(\frac{(v_1-v_2)(x_2-x_3)-(v_2-v_3)(x_1-x_2)}{(y_1-y_2)(x_2-x_3)-(y_2-y_3)(x_1-x_2)} \right)^2}{\left(\frac{(u_1-u_2)(y_2-y_3)-(u_2-u_3)(y_1-y_2)}{(x_1-x_2)(y_2-y_3)-(x_2-x_3)(y_1-y_2)} \right)^2 + \left(\frac{(v_1-v_2)(x_2-x_3)-(v_2-v_3)(x_1-x_2)}{(y_1-y_2)(x_2-x_3)-(y_2-y_3)(x_1-x_2)} \right)^2} \right) + \frac{E}{2(1+\nu)} \left(\frac{(u_1-u_2)(x_2-x_3)-(u_2-u_3)(x_1-x_2)}{(y_1-y_2)(x_2-x_3)-(y_2-y_3)(x_1-x_2)} + \frac{(v_1-v_2)(y_2-y_3)-(v_2-v_3)(y_1-y_2)}{(x_1-x_2)(y_2-y_3)-(x_2-x_3)(y_1-y_2)} \right)^2 \right] \quad (7)$$

2.3 Internal energy of triangular truss element

There exists a triangular truss element that has the same behaviour as the triangular plane element, as shown in Figure 2.

When the cross-sectional areas of members of a triangular truss element are assumed to be $A_1, A_2,$ and $A_3,$ the internal energy of the element in the state of a two-dimensional plane stress can be obtained with following equation:

$$U_T = \frac{1}{2} E\varepsilon_1^2 A_1 \ell_1 + \frac{1}{2} E\varepsilon_2^2 A_2 \ell_2 + \frac{1}{2} E\varepsilon_3^2 A_3 \ell_3 \quad (8)$$

where, U_T is the internal energy of the triangular truss element; $\varepsilon_1, \varepsilon_2, \varepsilon_3,$ and $A_1, A_2, A_3,$ and ℓ_1, ℓ_2, ℓ_3 are the deformed strains, and cross-sectional areas, and lengths of the triangular truss members 1, 2, and 3, respectively.

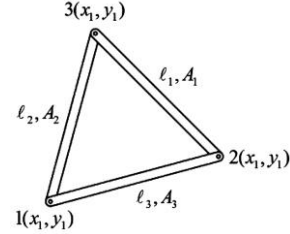


Figure 2 Triangular truss element

To determine the relationship between the cross-sectional area of each member and the weighted area associated with each member, and to find the conditions where the discretized truss element has the same behaviour as the continuum solid element, weighted areas (with regard to their center of gravity 'G') are introduced, and the weighted areas ($A'_1, A'_2,$ and A'_3) are identical to each other. Therefore, the following relationship can be induced as:

$$A_1 = A_2 = A_3 = nA \quad (9)$$

where, n is any multiple.

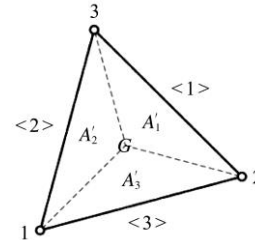


Figure 3 Weighted areas of triangular truss element

Finally, the internal energy of the triangular truss element can be obtained by substituting Equation (8) with the deformed strains of each truss member induced geometrically from Figure 2.

$$U_T = \frac{1}{2} E \left\{ \frac{\sqrt{\{(x_2+u_2)-(x_3+u_3)\}^2 + \{(y_2+v_2)-(y_3+v_3)\}^2} - \sqrt{(x_2-x_3)^2 + (y_2-y_3)^2}}{\sqrt{(x_2-x_3)^2 + (y_2-y_3)^2}} \right\}^2 nA\ell_1 + \frac{1}{2} E \left\{ \frac{\sqrt{\{(x_1+u_1)-(x_3+u_3)\}^2 + \{(y_1+v_1)-(y_3+v_3)\}^2} - \sqrt{(x_1-x_3)^2 + (y_1-y_3)^2}}{\sqrt{(x_1-x_3)^2 + (y_1-y_3)^2}} \right\}^2 nA\ell_2 + \frac{1}{2} E \left\{ \frac{\sqrt{\{(x_1+u_1)-(x_2+u_2)\}^2 + \{(y_1+v_1)-(y_2+v_2)\}^2} - \sqrt{(x_1-x_2)^2 + (y_1-y_2)^2}}{\sqrt{(x_1-x_2)^2 + (y_1-y_2)^2}} \right\}^2 nA\ell_3 \quad (10)$$

2.4 Relationship between continuum and discretized structures

The internal energies of triangular plane (solid structure) and triangular truss (discretized structure) elements can be calculated using Equations (7) and (10), respectively. If the geometries of both structural elements resisting external forces are deformed in the elastic range, and both the internal energies have the same value, it is possible to substitute the solid element with the discretized element. To apply the equivalence principle for the internal energies of the solid and discretized elements, it is necessary to rearrange the equations in terms of arbitrary variables: displacements u and v . However, since the displacements of the triangular truss element in the internal energy equation are represented as square roots, it is required to continue to square both sides of the energy equivalence equation until the square roots disappear.

Because this repeated process to eliminate the square roots is complicated, the Runge-Kutta method, which is generally used to find approximate solutions, was adopted instead. This analysis method found the volume ratio n that makes the two internal energy equations equal for any variables u and v under a fixed Poisson's ratio ν . When Poisson's ratio is 3^{-1} for ideal materials of isotropic and homogeneous nature, and 0.2 for materials with a brittle nature (such as concrete), the volumetric ratios n were determined to be 2.79036 and 2.79168, respectively.

Because the equivalent truss structure model used in this study originates from the Laplace equation $\nabla^2\phi = 0$, and the variables belonging to it are governed by a linear relationship, the regression equation between Poisson's ratio (ν) and the volumetric ratio (n) should follow a linear relationship. In the regression analysis, the volumetric ratio and Poisson's ratio showed an exact linear-relationship, as shown in Table 1.

Table 1 Poisson's ratio (ν) vs. volumetric ratio (n) of the triangular truss element to the triangular solid element

ν	n
0.2	2.79168
0.3	2.79069
1/3 (0.33)	2.79036
0.4	2.78970
0.5	2.78872

Note: $n = -0.00987\nu + 2.79365$.

3 Criteria

The model needs to determine special failure criteria and numerical procedures to apply to crack propagation and reliability analysis. Detailed explanations of the model are included in the following sections.

3.1 Loads

Only static loads such as weights loaded on the surfaces of a rigid body or very slowly moving loads acting on a sample laid on a universal testing machine (UTM) for a long time were assumed.

3.2 Tension

Because structural elements generally have material uncertainties, a safety factor for taking uncertainties of material into account should be considered. The allowable stress of an element is given by the following equation.

$$\sigma_{allow} = n \times \sigma = n \times \frac{P}{A_c} \tag{11}$$

where, σ_{allow} is the allowable stress; n is the safety factor (safety margin); σ is the internal stress; P is the external load; A_c is the internal cross section area of the material. A safety factor was not included in this study because it made the structural analysis method too complex. It is also assumed that the characteristics of variables are given as a type of distribution with average and standard deviation. When a static tension load is applied to ideal materials such as steel, for which Poisson's ratio is 0.3, a typical stress-strain curve is shown in Figure 4. Each node of the equivalent truss structure element for structural analysis in this study already consists of a hinge; therefore, it is supposed that the structural materials to resist the tension yield when the internal stresses of the elements reach a proportional stress limit.

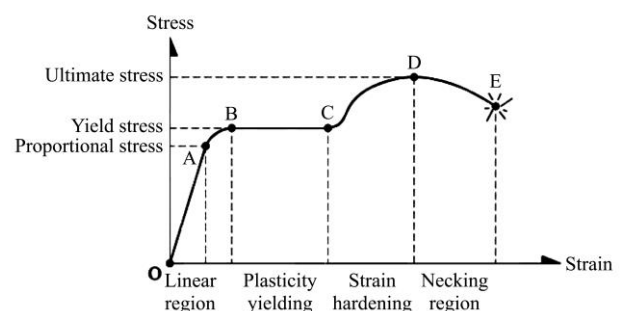


Figure 4 Typical stress-strain curve of material with Poisson's ratio of 0.3

3.3 Compression

If the element loaded axially in compression is a relatively slender structure, the structural component may buckle due to bending or lateral deflection before the internal stress reaches its allowable compressive stress. To check the slenderness (λ) which refers to the eccentric ratio between the effective length (l) of a column and the least radius of gyration (r) of its cross section, it is necessary to classify the structural members into long and short columns before applying the criteria for compression. The slenderness can be expressed by Equation (12).

$$\lambda = \frac{k\ell}{r} = \ell \sqrt{\frac{A}{I}} \quad (12)$$

where, k is the effective length factor; A is the cross sectional area; I is the moment of inertia of the area.

The effective length factor k is 1 because each node of the equivalent truss structure model consists of a hinge. If the qualities of irregular triangle meshes consisting of a whole domain are high enough for three sides of the triangle meshes to have the same length, the areas of the triangle meshes can be calculated by Heron's formula as follows (Figure 5).

$$A' = \sqrt{s(s-a)(s-b)(s-c)} = \frac{\sqrt{3}}{4} a^2 \quad (13)$$

where, A' is the area of irregular triangle mesh; s is $\frac{(a+b+c)}{2}$ and a is the length of one side of the triangular mesh.

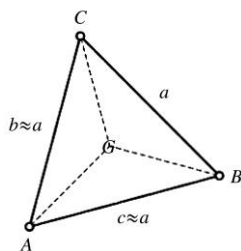


Figure 5 Irregular triangle mesh with side lengths of a , b and c

The volume ratio (n) is based on the assumption that the ratio is the volume of each truss element consisting of the triangular mesh to the volume of each triangular solid element divided by the gravity center of the whole solid element (Figure 6).

If the thickness of the solid element is t and the length of one side of the sectional area of each truss element is h ,

the h can be expressed as follows.

$$h = \sqrt{n \frac{A' t}{3 a}} = \sqrt{\frac{n \sqrt{3}}{3 \cdot 4} at} = \sqrt{\frac{n}{3} \frac{\sqrt{3}}{2}} \sqrt{at} \quad (14)$$

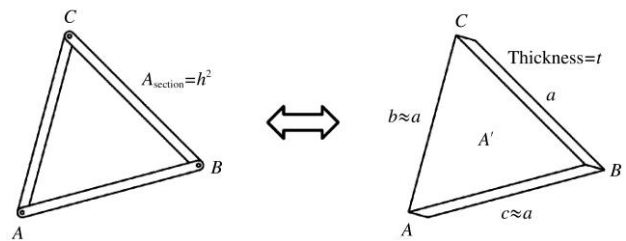


Figure 6 Truss element vs. solid element

Using Equation (14), the slenderness of the equation (12) can be obtained as follows.

$$\lambda = \ell \sqrt{\frac{A}{I}} = a \sqrt{\frac{\left(\frac{n \sqrt{3}}{3 \cdot 4} at\right)}{\frac{1}{12} \left(\frac{n \sqrt{3}}{3 \cdot 4} at\right)^2}} = \sqrt{12} \sqrt{\frac{3}{n}} \frac{2}{\sqrt{\sqrt{3}}} \sqrt{\frac{a}{t}} \quad (15)$$

The compatibility condition of the equivalent truss structure model implies that the volume ratio (n) is over 2 (Table 1). If the length (a) of one side of the triangular mesh is shorter than the thickness (t) of the solid element, the range of slenderness is given below.

$$\lambda \leq 6.45 \quad (16)$$

3.4 Examination of short and long columns

According to the design criteria of the American Concrete Institute (ACI), the critical slenderness ratio of a column not braced against a side sway can be expressed as follows.

$$\frac{k l_u}{r} \leq 22 \quad (17)$$

where, l_u is the length of the column not braced against the side sway.

According to the design criteria of the American Institute of Steel Construction (AISC), the critical slenderness ratio of a column not braced against a side sway can be defined as the ratio corresponding to 50% of the yield stress in Euler's curve when residual stress is considered as shown below.

$$\left(\frac{k\ell}{r}\right)_c = \sqrt{\frac{2\pi^2 E}{\sigma_y}} \quad (18)$$

where, E is the elastic modulus, MPa and σ_y is the yield stress, MPa.

The critical slenderness ratio of ideally elastic

material such as steel with an elastic modulus of 200 GPa and yield stress of 1000 MPa can be calculated as follows:

$$\left(\frac{k\ell}{r}\right)_c = 35 \quad (19)$$

Therefore, if the structure consists of practical construction materials such as concrete and steel, the equivalent truss structure model always satisfies the conditions of the short column.

3.5 Structural stability

If the global stiffness matrix, which is established by assembling the local stiffness matrices, has an inverse matrix while the structural topology is transformed from stable state to unstable state, the structure is either a statically indeterminate or determinate structure and there should be a unique solution to satisfy the relationship between the global stiffness matrix and the displacements of nodes. Therefore, the determinant of the structure can be used as a failure criterion to determine if the structure will collapse or not.

3.6 System collapse

It takes numerous computations to verify the stability of the collapsing structure by calculating the determinant of the global stiffness matrix whenever some cracks propagate during each time step. If the original structure has various boundary conditions, each structure separated from the collapsing structure could be an independent structure depending on some cases such as the situations shown in Figure 7.

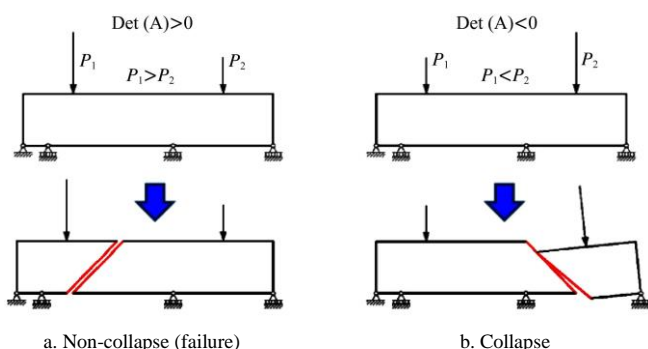


Figure 7 Non-collapse and collapse of statically indeterminate structure according to load conditions

The designer decides that those independent structures are statically indeterminate or determinate structures because the determinants of the structures are still positive. If there are no induced loads on the separated structures, the displacements of the structures

will be zero and then the structure will be regarded as stable.

Therefore, newly defined criteria to determine the systematic collapse were made on the assumption that the displacements at some nodes of the original structure are suddenly larger than the displacements that occurred in the previous step or become zero.

4 Probability analysis

4.1 Sampling

If the virtual experiments are repeated often enough to replace the probability variables with a normal distribution and the structural stability is determined by checking the limit state equations which define the collapse conditions of structure, the collapse probability can be calculated approximately. The Monte-Carlo sampling technique is a representative method. It is generally suggested that the total sampling number might be over 10-100 of the reciprocal of the expected collapse probability as shown in Equation (20) or should be large enough to guarantee the accuracy of the expected collapse probability.

$$N \geq \frac{10 \text{ to } 100}{P_f} \quad (20)$$

where, N is the total sampling number and P_f is the collapse probability.

Because the minimum sampling numbers can vary depending on the situation, such as the shape of the structure, the condition of the loads and boundary conditions, the relative errors between previous and current values of collapse probability were also checked.

4.2 Random variables

It was assumed that the characteristics of variables related to materials (resistances) and forces (loads) followed a standard normal distribution. A computer can produce random numbers from a long sequence that it creates. These numbers are called pseudo-random numbers. Because a set of this sequence relies on a designated number called 'seeds' of which the time corresponds to 1/1000 s, the computer can create different random numbers as often as desired. To create random numbers between 0 and 1, the random function embedded in Java™ (Oracle Corporation, Redwood Shores, CA,

USA) was called out recursively. Box-Muller functions as shown in Equations (21) and (22) transformed the random numbers created by the computer into a standard normal distribution^[39].

$$U_1 = (-2.0\ln(X_1))^{1/2} \times \cos(2\pi X_2) \quad \text{if } X_3 \geq 0.5 \quad (21)$$

$$U_2 = (-2.0\ln(X_1))^{1/2} \times \sin(2\pi X_2) \quad \text{if } X_3 < 0.5 \quad (22)$$

where, U_1 and U_2 are the non-associated standard normal random numbers; X_1 , X_2 and X_3 are the random numbers occurring between zero and one.

The targeted normal distribution can be obtained as shown in Equation (23):

$$X = \mu_x + \sigma_x \times (U_1 \text{ or } U_2) \quad (23)$$

where, X is the targeted normal distribution; μ is the mean and σ is the standard deviation.

4.3 Progressive elimination method

When external loads act on a structure, internal stresses occur at components of the structure following the stress paths produced by external loads. If the internal stresses are over the yield stresses, the components collapse and the extra stresses are redistributed to neighboring components in order to balance the structure. These processes will continue until the structure is stable. It is also assumed that the loads dealt with in this study are static loads which are gradually increased or relatively constant during the simulation. Therefore, the progressive elimination method, which sequentially removes the structural components with the largest stresses over the allowable stresses at each time step of the structural analysis, was adopted. However, if there were no redundant components to withstand the external loads during the processes, the structure was regarded as a collapsed structure. The detailed procedure is shown in Figure 8.

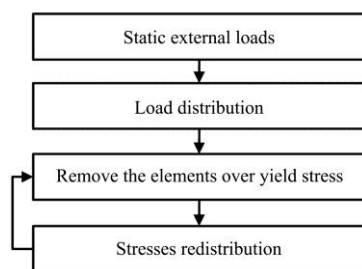


Figure 8 Progressive elimination method

4.4 Expression of removed components

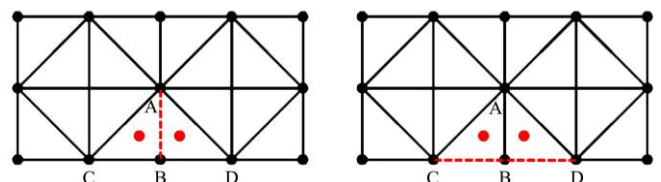
There are two methods of removing structural

components: actually removing the components or virtually making material properties of the removed components zero. Generally, the former method allows control of the input and output files. This approach occupies a considerable amount of computational time compared with the computational time needed for structural analysis. Therefore, the latter method was chosen to improve computational speed.

4.5 Removal of unnecessary members as structural components

When truss members with stresses larger than the yield stress are sequentially removed, truss members shown to be unnecessary as structural components are eliminated during the progressive elimination processes. In Figure 9a, the member AB is removed and the members BC and BD share the node B; the triangle ACD is unstable. In Figure 9b, the members BC and BD are removed; the member AB becomes unnecessary as a structural component. Therefore, structural analysis at each time step was carried out after removing all unnecessary members during the progressive elimination processes. The rule to remove unnecessary members is summarized below.

- 1) Remove any member exceeding the allowable stresses.
- 2) Select triangles that share with the member (triangles including the red dots as shown in Figure 9).
- 3) Check if there are triangles to share with any remaining sides of the selected triangles or not. If there are none, then remove other members connected with the removed members.
- 4) Repeat the same elimination processes for all removed members.



a. The case that the member AB is removed
 b. The case that the members BC and BD are removed

Figure 9 Unnecessary members as structural components

5 Results and discussion

Beams with various types of loads and boundary conditions were used to test the equivalent truss structure

model by executing crack propagation and calculating failure probability.

5.1 Simply supported beam with a concentrated load

A crack propagation test was conducted, changing the sizes and triangulation methods of the irregular triangle mesh. A simply supported beam with a concentrated load on the top middle point as shown in Figure 10 was considered for the test.

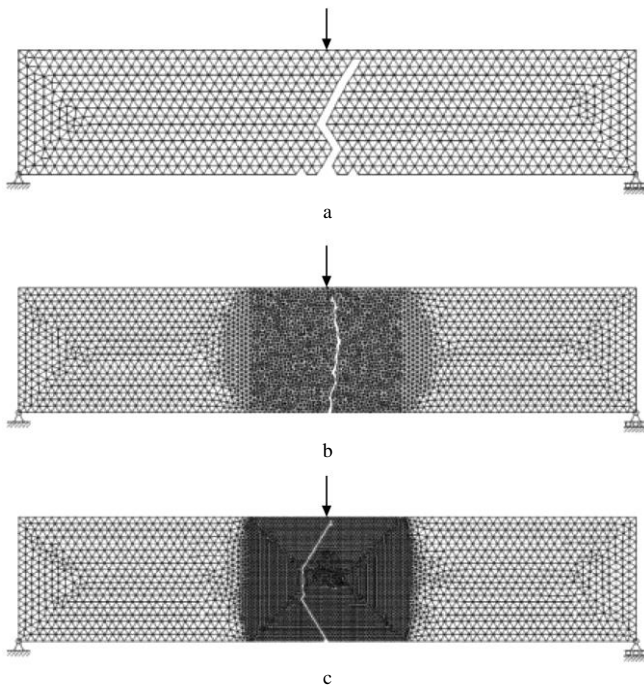


Figure 10 Crack propagation patterns of the structure using the coarse (a) vs. dense meshes using Delaunay-triangulation-based (b) and advancing front techniques (c), respectively

The beams had the following characteristics: width of 0.9 m, depth of 1.8 m, span length of 9.0 m, elastic modulus of 20.0 GPa, concentrated load of 25 kN with standard deviation of 2 kN, and resisting moment of 60 kN m with a standard deviation of 6 kN m. The coarse meshes consisted of 980 nodes and 2793 elements were uniformly distributed over the whole domain as shown in Figure 10a. However, since it is already known that the crack propagation of the beam occurs at the mid area of the span, it is possible to increase the mesh density using dense meshes across the area to reduce the computational time. For the other beams with different types of mesh conditions in the area, the whole domain was divided into 9326 elements including 3181 nodes and 14080 elements including 4782 nodes using Delaunay-triangulation-based and advancing front techniques, respectively. In the case of the coarse mesh, the crack developed in the wrong

direction. Even the dense mesh constructed by the advancing front technique was suboptimal because the meshes were not distributed consistently through the mid domain. On the other hand, the case created by the Delaunay-triangulation-based technique demonstrated desirable crack propagation.

The failure probability of the structure based on the Delaunay triangle mesh was calculated as shown in Table 2. An analytical solution for failure probability based on the limit state equation expressed in the form of a moment was 30.85% (Thoft-Christensen and Murotsu, 1986). It was understood that the approximate solution of the failure probability was closer to the analytical solution as the sampling number increased.

Table 2 Failure probability of simply supported beam under a concentrated load

Sampling number	Failure probability
800	0.2931
2400	0.2974

5.2 Crack propagation of a beam subjected to multiple boundary conditions

The experimental result of crack development in concrete was compared with the regular and irregular truss structure model equivalent to the continuum^[40]. The dimensions and material properties of the structure subjected to multiple boundary conditions are shown in Figure 11 and Table 3. In the case of the irregular truss structure, the region in which the crack occurred was filled with dense mesh to reduce computational time, whereas the whole domain of the regular truss structure was divided into sizes which were equal to the sizes of the dense meshes of the irregular truss structure. There were 5611 nodes and 18140 elements, and 1994 nodes and 5766 elements used for the regular and irregular truss structures, respectively.

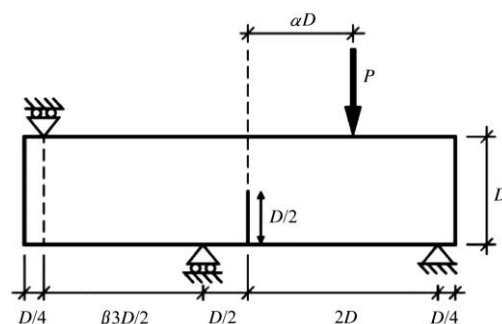


Figure 11 Beam subjected to multiple boundary conditions

Table 3 Dimensions and material properties of beam

Variables	Values	Units	Description
D	150.00	mm	Depth of beam
t	50.00	mm	Thickness of beam
L	675.00	mm	Span length of beam
α	1.00		Constant
β	1.00		Constant
W	7.50	mm	Width of notch
P	13.00	kN	Point load
E	38.40	GPa	Young's modulus
ν	0.33		Poisson's ratio
ℓ	7.50	mm	Length of regular truss element

The simulation results of cracks propagated during 66 steps of testing are shown in Figure 12. It took 675 min and 167 min to complete the crack simulations of the regular and irregular truss structures, respectively.

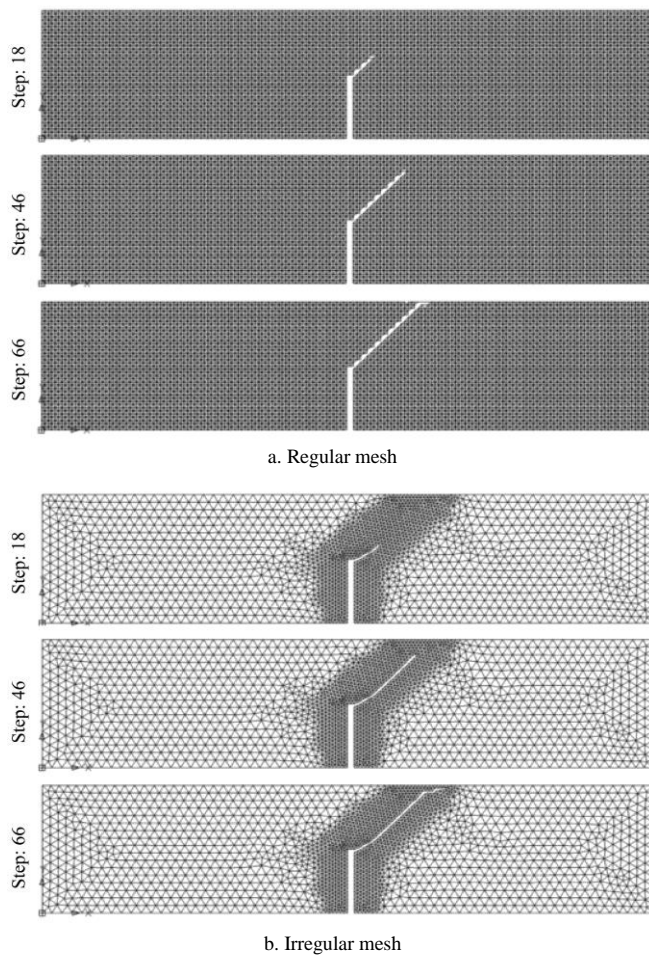


Figure 12 Crack propagations of regular (a) and irregular (b) truss structure models equivalent to continuum

The crack pattern of the regular truss structure was in a straight line, whereas the crack shape of the irregular truss structure followed a curvilinear form. The ability to break away from the main route of the crack was observed at both the beginning and end times. Research on fracture mechanism was started by Griffith, and glass

was used for most experiments that included tensile tests^[41,42]. Tensile stress could be a main reason for the fracture. Brittle materials are fractured in a trans-crystalline direction, and some cracks changed their forward direction instantly from the surface of a structure to the inside. It was also shown in other research that a fracture in brittle material occurs in the vertical direction when tensile stresses exist^[43]. These observations are in good agreement with the simulation results of the irregular truss structure model developed in this study.

5.3 Simply supported beam with two independent concentrated loads

A simply supported beam with two independent concentrated loads was tested to evaluate the feasibility of an irregular truss structure model for crack propagation and probability analysis as shown in Figure 13.

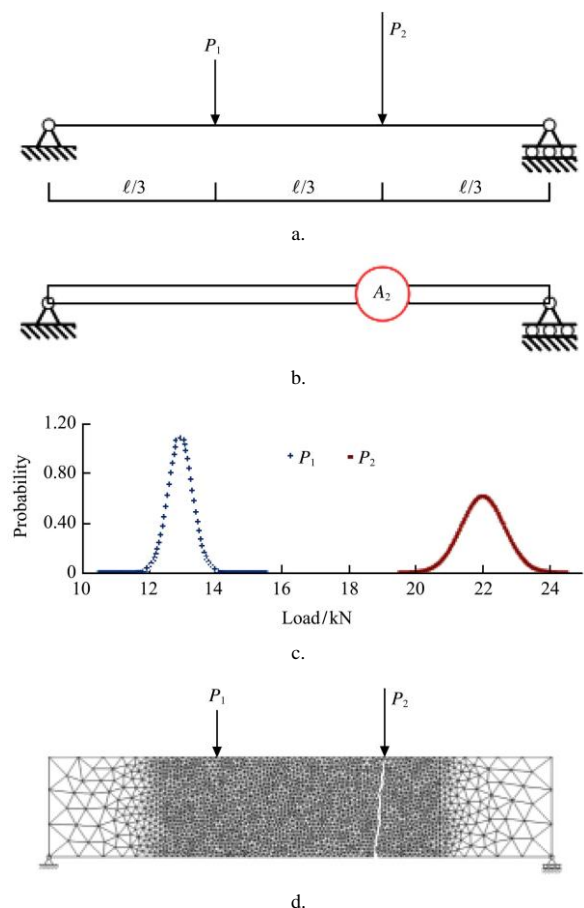


Figure 13 Case that there is no overlapping area between each distribution of two concentrated independent loads; it represents the locations of loads (a), the possible area of collapse (b), the probabilities of loads (c) and the pattern of crack propagation (d)

The beams had the following characteristics: width of 0.9 m, depth of 1.8 m, span length of 9.0 m, elastic modulus of 20.0 GPa, concentrated load P_1 of 12.94 kN

with standard deviation of 0.37 kN, concentrated load P_2 of 21.99 kN with standard deviation of 0.65 kN, and resisting moment of 60 kN m with standard deviation of 6 kN m. The only mid area consisted of a dense mesh and the whole domain was divided into 6643 elements including 2260 nodes.

Until the structure collapsed, the crack developed only at the area subjected to the larger load. The structure's failure probability was calculated as shown in Table 4. The analytical solution for failure probability based on the limit state equation expressed in the form of a moment was 30.85%. The approximate solution to failure probability was closer to the analytical solution as the sampling number increased. Therefore, it was verified that an approach using an equivalent truss structure model is sufficiently accurate to estimate the failure probability of the continuum structure.

Table 4 Failure probability when there is no overlapped area between each distribution of two concentrated independent loads

Sampling number	Failure probability
800	0.2861
2400	0.2892

In this time, the special case that the distributions of the loads P_1 and P_2 dealt with in the above example were overlapped by changing the means and standard deviations of the loads was considered. The loads included the following details: the concentrated load P_1 of 17.97 kN with a standard deviation of 4.00 kN and load P_2 of 18.97 kN with a standard deviation of 0.60 kN. To obtain the analytical solution for failure probability, the first conditional case in which load P_1 is bigger than load P_2 was assumed (Figures 14 and 15a):

$$M_{\max} = \frac{1}{9}(2P_1 + P_2)\ell = \frac{1}{9}P\ell \quad (24)$$

where, $\mu_p = 2\mu_{P_1} + \mu_{P_2}$, $\sigma_p^2 = 2^2\sigma_{P_1}^2 + \sigma_{P_2}^2$, and M_{\max} is the maximum moment that occurs due to the combination of loads.

The limit state equation could be expressed in the form of a moment as follows:

$$g = M_R - M_{\max} = M_R - \frac{1}{9}P\ell \quad (25)$$

where, $\mu_g = \mu_{M_R} - \frac{\ell}{9}\mu_p$, $\sigma_g^2 = \sigma_{M_R}^2 + \left(\frac{\ell}{9}\right)^2\sigma_p^2$, and M_R

is the resisting moment.

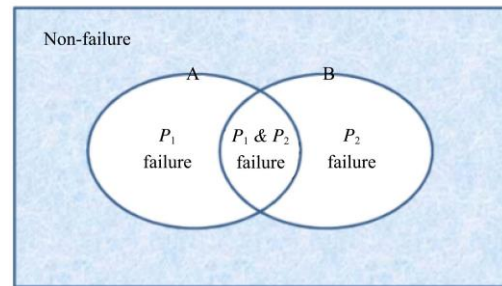


Figure 14 Venn diagram of loads P_1 and P_2

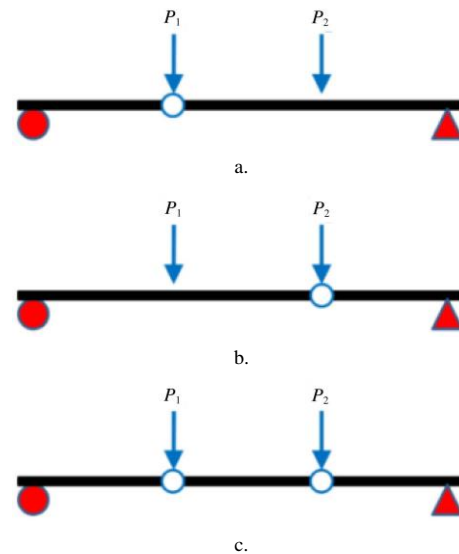


Figure 15 Various failure modes according to the load conditions: collapses of node 1 (a), node 2 (b), and both nodes 1 and 2 (c) due to load P_1 , load P_2 , and both loads P_1 and P_2 , respectively

The failure probability P_{f1} was calculated to be 0.31 from the reliability index β of the limit state equation. The second conditional case in which the load P_2 is bigger than P_1 was assumed (Figures 14 and 15b). The failure probability P_{f2} was calculated to be 0.29 as in the previous case.

From the Venn diagram shown in the Figure 14, the failure probability (P_f) of the structure can be set up following the intersection rule of the Venn diagram.

$$P_f = P(A) + P(B) - P(A \cap B) \quad (26)$$

From the Figure 14, the probability for only node 1 to collapse due to the load P_1 can be defined as below:.

$$P(A) = P_{f1}(1 - P_{f2}) \quad (27)$$

The probability for only node 2 to fail due to load P_2 can be induced by applying the same method.

$$P(B) = (1 - P_{f1})P_{f2} \quad (28)$$

The probability for nodes 1 and 2 to collapse simultaneously due to loads P_1 and P_2 is defined below.

$$P(A \cap B) = P_{f1} \cdot P_{f2} \quad (29)$$

From Equations (26) to (29), the failure probability of the structure was calculated to be 32.95%. The simulation results using the equivalent irregular truss structure model showed that the probabilities were 40.42%, 24.63%, 10.08% and 34.71% in the cases where the load P_1 is greater than P_2 without regard to structural failure; only node 1 collapses due to load P_1 ; only node 2 collapses due to load P_2 , and nodes 1 or 2 collapse due to both loads P_1 and P_2 , respectively (Table 5). Two kinds of failure modes were also observed because the loads systematically affected each other (Figure 16).

Table 5 Failure probability in the case that there is an overlapped area between each distribution of two concentrated independent loads

Sampling number	Failure probability			Analytical solution
	$P_1 > P_2$	$P_1 < P_2$	$P_1 > P_2$ or $P_1 < P_2$	
800	0.2550	0.0988	0.3538	0.3295
2400	0.2463	0.1008	0.3471	

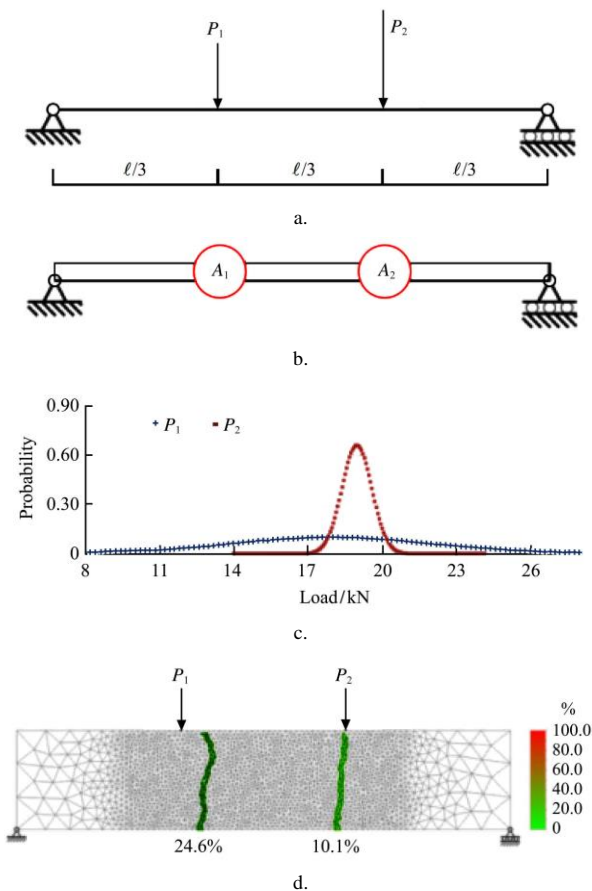


Figure 16 Case in which there is an overlapping area between each distribution of two concentrated independent loads; it represents the locations of loads (a), the possible areas of collapse (b), the probabilities of loads (c) and the patterns of crack propagation (d)

6 Conclusions

A discretized model that shows the same behaviour as a continuum structure, referred to as the equivalent truss structure model, was developed based on irregular triangle elements. With the assumptions that displacements occurred in a two-dimensional plane, the deformation maintained a linear relationship, and the size of the element was infinitesimal enough to have all stresses at any location inside the domain be identical, the energy conservation theory was applied to obtain the necessary conditions for the equivalent truss structure model. The volumetric ratio of the truss element to the solid element showed an exact linear relationship because this model was based on the Laplace equation. The detailed rules and processes for the crack propagation and reliability analysis of an irregular truss structure model were also developed. Through various examples, it was proved that the equivalent truss structure model is useful for simulation of crack propagation and estimating the failure probability of the continuum structure. The uncertainty imbedded in the irregular triangle meshes could describe the propagation of a crack more realistically. The model could also be expanded for three-dimensional structure analysis. This model can be used for the simulations of crack propagation and reliability analysis in the areas of agricultural engineering related to structure, soil, food and so on. However, the model in this study assumes that a crack propagates statically. Therefore, if the amount of deformation of a structure exceeds the elastic range during the crack propagation processes, the crack propagation model would be inaccurate. Therefore, in the future, it will be necessary to further develop the amended model to include the dissipation energy associated with crack propagation.

Acknowledgment

The work was supported by research grants of Seoul National University, and Chungbuk National University.

[References]

- [1] Neville A M. Properties of concrete. New York, NY: John Wiley and Sons, 1996.
- [2] Park R, Paulay T. Reinforced concrete structures. New York, NY: John Wiley and Sons, 1975.
- [3] Corotis R B. Probability-based design codes. *Concr. Int.*, 1985; 7(4): 42–49.
- [4] Hasofer A M, Lind N C. Exact and invariant second-moment code format. *J. Eng. Mech. Div., ASCE*, 1974; 100(1): 111–121.
- [5] Cornell C A. Bounds on the reliability of structural systems. *J. Struct. Div., ASCE*, 1967; 93(1): 171–00.
- [6] Freudenthal A M. Safety and the probability of structural failure. *T. ASCE*, 1956; 121(1): 1337–1397.
- [7] Shinozuka M. Basic analysis of structural safety. *J. Struct. Div., ASCE*, 1983; 109(3): 721–740.
- [8] Rackwitz R, Fiessler B. Note on discrete safety checking when using non-normal stochastic models for basic variables. Loads Project Working Session. Cambridge, MA: MIT. 1976.
- [9] Rackwitz R, Fiessler B. Structural reliability under combined random load sequences. *Comput. Struct.*, 1978; 9(5): 489–494.
- [10] Hohenbichler M, Rackwitz R. Non-normal dependent vectors in structural safety. *J. Eng. Mech. Div., ASCE*, 1981; 107(6): 1227–1238.
- [11] Rosenblatt M. Remarks on a multivariate transformation. *Ann. Math. Stat.*, 1952; 23(3): 470–472.
- [12] Fiessler B, Rackwitz R, Neumann H J. Quadratic limit states in structural reliability. *J. Eng. Mech. Div., ASCE*, 1979; 105(4): 661–676.
- [13] Breitung K. Asymptotic approximations for multinormal integrals. *J. Eng. Mech. Div., ASCE*, 1984; 110(3): 357–366.
- [14] Madsen H O, Krenk S, Lind N C. Methods of structural safety. Englewood Cliffs, NJ: Prentice-Hall, Inc. 1986.
- [15] Tvedt L. Two second-order approximations to the failure probability. Section on Structural Reliability. Hovik, Norway: A/S Vertas Research. 1984.
- [16] Tvedt L. On the probability content of a parabolic failure set in a space of independent standard normally distributed random variables. Section on Structural Reliability. Hovik, Norway: A/S Vertas Research. 1985.
- [17] Kiureghian A D, Lin H Z, Hwang S J. Second-order reliability approximations. *J. Eng. Mech. Div., ASCE*, 1986; 113(8): 1208–1225.
- [18] Lee J. Reliability analysis modeling of frame structures based on discretized ideal plastic method. PhD dissertation. Seoul, South Korea: Seoul National University, 1991, 2.
- [19] Park S. System reliability analysis of reinforced concrete frames. PhD dissertation. Seoul, South Korea: Seoul National University, 1992, 2.
- [20] Yang Y, Kim J. Probabilistic finite element analysis of plane frame. *J. Comput. Struct. Eng. Inst. Korea*, 1989; 2(4): 89–98.
- [21] Handa K, Anderson K. Application of finite element methods in stochastic analysis of structures. Proc. 3rd Intl. Conf. Structural Safety and Reliability. New York, NY: IASAR. 1981.
- [22] Ang A H-S, Amin M. Studies of probabilistic safety analysis of structures and structural systems. Urbana, IL: University of Illinois. 1967.
- [23] Ishizawa J. On the reliability of indeterminate structural systems. PhD dissertation. Urbana, IL: University of Illinois, 1968.
- [24] Stevenson J, Moses F. Reliability analysis of frame structures. *J. Struct. Div., ASCE*, 1970; 96(11): 2409–2427.
- [25] Gorman M. Automatic generation of collapse mode equation. *J. Struct. Div.*, 1981; 107(7): 1350–1354.
- [26] Ma H-F, Ang A H-S. Reliability analysis of redundant ductile structural systems. Urbana, IL: University of Illinois. 1981.
- [27] Moses F. System reliability developments in structural engineering. *Struct. Saf.*, 1982; 1(1): 3–13.
- [28] Moses F, Stahl B. Reliability analysis format for offshore structures. Proc. the 10th Ann. Offshore Technology Conference. Houston, TX: OTC. 1978.
- [29] Murotsu Y, Okada H, Taguchi K, Grimmelt M, Yonezawa M. Automatic generation of stochastically dominant failure modes of frame structures. *Struct. Saf.*, 1984; 2(1): 17–25.
- [30] Thoft-Christensen P, Murotsu Y. Application of structural systems reliability theory. New York, NY: Springer-Verlag. 1986.
- [31] Ditlevsen O, Bjerager P. Reliability of highly redundant plastic structures. *J. Eng. Mech., ASCE*, 1984; 110(5): 671–693.
- [32] Grimmelt M, Schueller G I. Benchmark study on methods to determine collapse failure probabilities of redundant structures. *Struct. Saf.*, 1982; 1(2): 93–106.
- [33] Melchers R E. Structural system reliability assessment using directional simulation. *Struct. Saf.*, 1994; 16(1-2): 23–37.
- [34] Moses F, Fu G. Important sampling in structural system reliability. Proc. the 5th ASCE-EMD/GTD/STD Specialty Conf. Probabilistic Mechanics. Reston, VA: ASCE. 1988.
- [35] Rashedi M R. Studies on reliability of structural systems. PhD dissertation. Cleveland, OH: Case Western Reserve University, 1984.

- [36] Corotis R B, Nafday A M. Structural system reliability using linear programming and simulation. *J. Struct. Eng.*, ASCE, 1989; 115(10): 2435–2447.
- [37] Kim D. Matrix-based system reliability analysis using the dominant failure mode search method. PhD dissertation. Seoul, South Korea: Seoul National University, 2009, 2.
- [38] Melchers R E. Structural reliability, analysis and prediction. West Sussex, England: Ellis Horwood, 1987.
- [39] Box G E P, Muller M E. A note on the generation of random normal deviates. *Ann. Math. Stat.*, 1958; 29(2): 610–611.
- [40] Gávez J C, Elices M, Guinea G V, Planas J. Mixed mode fracture of concrete under proportional and nonproportional loading. *Int. J. Fracture*, 1998; 94(3): 267–284.
- [41] Griffith A A. The phenomena of rupture and flow in solids. *Philos. T. R. Soc. Lond.*, 1920; 221: 163–198.
- [42] Griffith A A. The Theory of rupture. *Proc. 1th Intl. Congr. Applied Mechanics*. New York, NY: John Wiley & Sons, Inc, 1924.
- [43] Irwin G R. Fracture mechanics. *Proc. the 1th Sym. Naval Structural Mechanics*. Elmsford, NY: Pergamon Press, 1956.